The Silica-Like Extended Polymorphism of Cobalt(II) Imidazolate Three-Dimensional Frameworks: X-ray Single-Crystal Structures and Magnetic Properties

Yun-Qi Tian,[a, c] Chen-Xin Cai,[a] Xiao-Ming Ren,[a] Chun-Ying Duan,[a] Yan Xu,[a] Song Gao,*[b] and Xiao-Zeng You*[a]

Abstract: Five polymorphous frameworks of cobalt(II) imidazolates (**1**–**5**) have been prepared by solvatothermal syntheses. Of these, compound **3** has already been synthesized in a gas-phase reaction by Seel et al. in 1969 and structurally characterized by Sturm et al. in 1975. The new synthetic strategy affords four polymorphous frameworks of cobalt(II) imidazolates (**1, 2, 4, 5**) of crystalline substances, of which the compound **4** ($a = b = 23.450(3)$, $c = 12.460(3)$ Å, tetragonal, $I4_1cd$, $Z = 16$) is an isomorphous compound of $[Zn(im)_2]_\infty$, which was also synthesized in a gas-phase reaction in 1980. The frameworks of compounds **1** and **2** are porous and isostructural; they have the same framework topology that represents a novel uninodal (6,4)-net: **1**: $a = 18.513(4)$, $b = 24.368(5)$, $c = 9.2940(19)$ Å, orthorhombic, $Fdd2$, $Z = 16$; **2**: $a = 17.635(4)$, $b = 27.706(6)$, $c = 9.0810(18)$ Å, orthorhombic, $Fdd2$, $Z = 16$. The framework of compound **5** exhibits a topology of zeolitic structure with the unit-cell parameters: $a = 24.3406(8)$, $b = 9.4526(3)$, $c = 24.8470(8)$ Å, $\beta = 91.977(1)°$, monoclinic, $P2_1/n$, $Z = 4$. All polymorphous frameworks of cobalt(II) imidazolates reflect the structural features of silica (SiO_2) and also exhibit different magnetic behaviors, although the imidazolates transmit the antiferromagnetic coupling between the cobalt(II) ions in all cases. However, the uncompensated antiferromagnetic couplings arise from spin-canting are sensitive to the structures: compound **1** is an antiferromagnet with $T_N = 13.11$ K; compounds **2**–**4** are weak ferromagnets (canted antiferromagnets): **2** shows a very weak ferromagnetism below 15 K, **3** exhibits a relatively strong ferromagnetism below 11.5 K and a coercive field (H_C) of 1800 Oe at 1.8 K, and **4** displays the strongest ferromagnetism of the three cobalt imidazolates and demonstrates a T_C of 15.5 K with a coercive field, H_C, of 7300 Oe at 1.8 K. However, compound **5** seems to be a hidden canted antiferromagnet with a magnetic ordering temperature of 10.6 K.

Keywords: cobalt · coordination polymers · magnetic properties · N ligands · zeolite analogues

Introduction

Metal-organic porous materials have attracted considerable attention in the last few years because of the promising applications in catalysis, separation, and molecular recognition.[1] However, the construction of open metal-organic frameworks still faces the challenge of increasing and modulating the size of pores to create more stable porous metal-organic materials. Although several approaches have been made to increase the pore size by enlarging the organic moieties, they often lead to instability or interpenetration of the frameworks.[2] Therefore, rational design and synthesis of open metal-organic frameworks are based on a significant motivation to avoid the above-mentioned defects. Recently, a breakthrough has been made in the creation of exceptionally stable and highly porous metal-organic frameworks by the use of secondary building units (SBU). Translating the SBUs into expanded open metal-organic frameworks has

[a] Prof. X.-Z. You, Prof. Dr. Y.-Q. Tian, Dr. C.-X. Cai, Dr. X.-M. Ren, Prof. Dr. C.-Y. Duan, Dr. Y. Xu
State Key Laboratory of Coordination Chemistry, Coordination Chemistry Institute
Nanjing University, Nanjing 210093 (P. R. China)
Fax: (+86) 25-3314502
E-mail: xyz@nju.edu.cn

[b] Prof. Dr. S. Gao
State Key Laboratory of Rare Earth Materials Chemistry and Applications
College of Chemistry and Molecular Engineering
Peking University, Beijing 100871 (P.R. China).
E-mail: gaosong@pku.edu.cn

[c] Prof. Dr. Y.-Q. Tian
Department of Chemistry, Liaoning University
Shenyang, 110036 (P. R. China)

 DOI: 10.1002/chem.200304957

been regarded as a key to imparting stability and rigidity into the resulting network and providing a means of preventing the formation of interpenetrated nets.[3] The strategy we used to a create stable and rigid metal-organic framework with large pores is based on expanding the zeolitic topologies by construction of metal-organic tetrahedral building blocks.[7] For the tetrahedral atoms (T) of zeolite we chose four-coordinate transition metals and for the linkers or vertices (X) of the T atoms we chose imidazolates. We expected that the resulting metal-organic polymer could have an open framework with zeolite or zeolite-like topology. The use of imidazolate as linker is not a random choice, but a deliberate selection since the two coordinating nitrogen atoms of imidazolate orientate with respect to each other at an angle of $\approx$144° which closely resembles the 145° angle of oxygen coordination in zeolites. Furthermore, the deprotonated imidazole is negatively charged so that the formed TX_2 compound would bear a strong resemblance to the structures of silica or zeolites: 1) If we chose transition metals M^{II} as T atoms, the electronic neutral frameworks of silica-like structures would be produced. 2) If some of the T atoms of M^{II} were replaced by the T atoms of M^{III}, the resulting framework would be similar to the aluminosilicate; however, here the frameworks were not charged negatively, but positively. 3) If some of the T atoms were replaced by O atoms (octahedrally coordinated metals) of M^{II} or M^{III}, the resulting frameworks would be analogous to those of the zeolite-like metallophosphates. And, if extended polymorphism occurred, we would make the metal imidazolates similar to silica, aluminosilicates, or metallophosphates. In addition, as infinite metal-organic frameworks constructed from transition metals and π-conjugated ligands, they could be potential candidates for electronic, optical, or magnetic materials. Therefore, the polymorphism of metal imidazolate frameworks would be not only an important motif for a new generation of porous materials, but also a significant topic for investigating the relationship between the framework structures and the physical properties of substances. Very recently, a structural and spectroscopic study on the polymorphism of copper(II) imidazolate polymers was reported.[4] Although the copper(II) imidazolates have already been investigated, the structural studies were limited to X-ray powder diffraction (XRPD) because of the lack of suitable single crystals. In addition, the XRPD method is only available if the complexity of the species is not too great and for monophasic crystalline powders.[5] Moreover, according to the XRPD results, the copper(II) imidazolate polymers did not display the open frameworks we expected; thus, we believe that a rational structural design of such porous compounds requires a logical synthetic strategy.

Imidazolates incorporating other polydentate ligands can form polynuclear complexes that are commonly used as bioinorganic model compounds. Therefore, these imidazolic complexes were prepared for the purpose of bioinorganic motifs.[6] Prior to our report on a porous framework of cobalt(II) imidazolate,[7] there had been only three different frameworks of metal imidazolates ($[Cu(im)_2]_\infty$,[8] $[Co(im)_2]_\infty$,[9] and $[Zn(im)_2]_\infty$[10]) that had been characterized by X-ray single-crystal studies. However, these crystalline compounds also did not display open frameworks. To create the metal imidazolate in a suitable crystalline size and with an open framework, we adopted the synthetic strategy applied for zeolites. After a series of experiments, we found that cobalt(II) is an ideal metal for the T atoms, and some of the alkyl alcohols are ideal solvents for the solvatothermal syntheses. Also, we applied various organic bases as structure-directing agents. To date, we have used our synthetic strategy to prepare at least five polymorphous frameworks of cobalt(II) imidazolates: three of them are open frameworks, of which one exhibits a zeolite-like topology.[7] Interestingly, the five polymorphous structures also display different magnetic behavior.

In the past 20 years, there have been a number of reports on magnetic studies of the imidazolate-bridged homobimetallic (or heterobimetallic) and oligometallic complexes,[6a–g] which reveal that the imidazolate linkage provides an efficient pathway for antiferromagnetic exchanges. Complex $[Cu(im)(imH)_2Cl]_x$, a 1D metal-organic polymer bridged by a single imidazolate, was reported to exhibit strong antiferromagnetic exchange.[11] In 1997, the structure and magnetic study of the 3D polymer $[Fe_3(im)_6(imH)_2]_x$[12] revealed that the imidazolates transmit antiferromagnetic coupling between the iron(II) ions, but with canted spin, leading to weak ferromagnetism at low temperatures. In the homopolymeric system of metal imidazolates $[M(im)_2]_\infty$, although the different polymorphs of $[Cu(im)_2]_\infty$[13] were magnetically studied and indicated the existence of antiferromagnetic interaction between the copper(II) ions through imidazolate linkages, the results were based nevertheless on the magnetic determination above 80 K. There has been no relevant magnetic study reported of the homopolymer $[Co(im)_2]_\infty$[9] reported by Sturm et al. Herein, we report the synthesis, X-ray single-crystal study, and magnetic properties of the five compounds with different polymorphous frameworks $[Co(im)_2]_\infty$, which display silica-like metal-organic structures. To facilitate the discussions in this paper, the five compounds are denoted **1** ($[Co(im)_2{\cdot}0.5\,Py]_\infty$, Py = pyridine), **2** ($[Co(im)_2{\cdot}0.5\,Ch]_\infty$, Ch = cyclohexanol), **3** ($[Co(im)_2]_\infty$, space group $I4_1$), **4** ($[Co(im)_2]_\infty$, space group $I4_1cd$), and **5** ($[Co_5(im)_{10}{\cdot}2\,MB]_\infty$, MB = 3-methyl-1-butanol).

Results

Synthesis of the cobalt(II) imidazolates with polymorphous frameworks: The compounds of cobalt imidazolates **1–5** were generally prepared by a solvatothermal method below 130–140 °C; however, the synthesis of each compound depends on the structure-directing agents and solvents (templates) used (Table 1).

Crystal structures of the five compounds: All cobalt(II) imidazolates reported here are crystalline materials (Table 2). Similar to inorganic silica, the compounds are generally formulated as $[Co(im)_2{\cdot}x\,G]$ (x = 0, 0.4 or 0.5; G = guest molecule) and are infinite 3D polymers with neutral frameworks in which the cobalt(II) ions are tetrahedrally coordinated and bridged by imidazolate ligands (Figure 1).

Table 1. Solvents and structure-directing agents used in the syntheses.[a]

SD	Ethanol	3-Methyl-1-butanol	Cyclohexanol	3-Methyl-1-hexanol	Pyridine
pyridine	3	1	1	1	1
piperazine	3	5	2	4	–
triethanolamine	unknown powder	unknown powder	unknown powder	4	–

[a] SD: structure-directing agent, SOL: solvent, –: the experiments were not carried out.

Table 2. Crystallographic data for compounds **1–5.**

	1	**2**	**3**	**4**	**5**
formula	$CoC_{8.5}H_{8.5}N_{4.5}$ $[Co(im)_2{\cdot}0.5\,Py]$	$CoC_9H_{12}N_{4.5}$ $[Co(im)_2{\cdot}0.5\,Ch]$	$Co_4C_{24}H_{24}N_{16}$ $[Co(im)_2]_4$	$Co_2C_{12}H_{12}N_8$ $[Co(im)_2]_2$	$Co_5C_{40}H_{54}N_{20}O_2$ $[Co(im)_2{\cdot}0.4\,MB]_5$
Fw	232.63	243.16	193.08×4	193.08×2	228.34×5
space group	*Fdd*2 (no. 43)	*Fdd*2 (no. 43)	$I4_1$ (no. 80)	$I4_1cd$ (no. 110)	$P2_1/n$ (no. 14)
crystal system	orthorhombic	orthorhombic	tetragonal	tetragonal	monoclinic
a [Å]	18.513(4)	17.635(4)	22.888(3)	23.450(3)	24.3406(8)
b [Å]	24.368(5)	27.706(6)	22.888(3)	23.450(3)	9.4526(3)
c [Å]	9.2940(19)	9.0810(18)	12.941(3)	12.460(3)	24.8470(8)
α [°]	90.00	90.00	90.00	90.00	90.00
β [°]	90.00	90.00	90.00	90.00	91.977(10)
γ [°]	90.00	90.00	90.00	90.00	90.00
V [Å^3]	4192.7(15)	4437.0(15)	6779(2)	6851.8(19)	5713.8(3)
Z	16	16	8	16	4
ρ [g cm^{-1}]	1.474	1.456	1.513	1.497	1.327
μ [mm^{-1}]	1.603	1.520	1.946	1.943	1.470
Flack	0.00	0.01	0.01	0.14	
$R^{[a]}$ [%]	4.02	3.73	5.18	3.66	6.88
$wR^{[b]}$ [%]	11.18	10.35	14.22	10.23	22.98

[a] $R = \Sigma(||Fo|-|Fc||)/\Sigma|Fo|$. [b] $wR = \{\Sigma w[(F_o^2-F_c^2)^2]/\Sigma w[(F_o^2)^2]\}^{1/2}$

*Compounds **1** and **2***: These two compounds are isostructural or can be regarded as supramolecular isomers (Figure 2).[14] They are constructed from the same metal ions and the same ligands, and crystallize in the same framework topology (Figure 1) with the same space group. However, they represent two different crystalline phases that can be distinguished from each other by their different unit cell parameters, framework openings, channel inclusions, and framework stabilities as well as their magnetic properties. The framework of **1** or **2** contains only a crystallographically unique cobalt(ii) ion and two independent imidazolate linkages (**1**: Co···Co 5.855–5.945 Å, N-Co-N angle 102.7–112.8°; **2**: Co···Co 5.860–6.007 Å, N-Co-N angle 105.5–113.2°). Within the framework, the cobalt ions are linked into boat- and chairlike 6-rings, which form an enclosed 6^6 cage unit (four chairlike rings around and two boatlike rings front and back along the *c* axis; Scheme 1). These 6^6 cage units (each accommodates a pyridine molecule in **1** and a cyclohexanol molecule in **2**) are linked to form an infinite 3D net with 1D channels of openings 5.3×10.4 Å in **1** and 6.6×8.4 Å in **2** along the *b* axis. This is an interesting net because of its close relationship to the cristobalite (diamond net with 6^4 cage unit) and tridymite structures (lonsdaleite net with 6^5 cage unit)[15a] (Scheme 1) that was first announced by O'Keeffe et al. in 1992[15b] and is demonstrated here in real crystal structures for the first time.

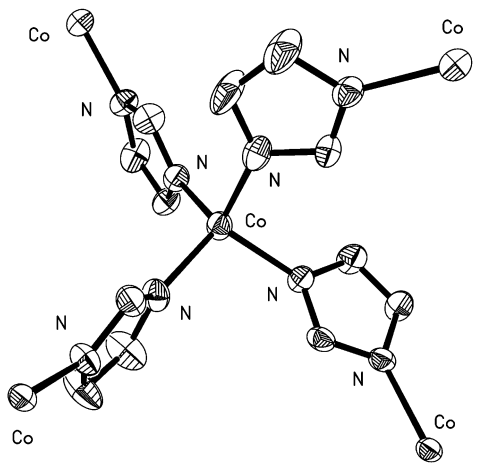

Figure 1. The cobalt(ii) coordination environment in the frameworks of cobalt imidazolates. The diagram was plotted based on compound **5** with thermal ellipsoids at 50% probability level.

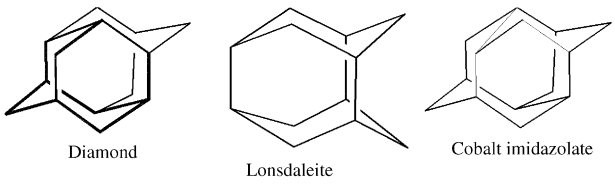

Scheme 1. Comparison of the diamond and lonsdaleite cage units with that of **1** (or **2**) to highlight the close relationship between structures of cristobalite, tridymite, and **1** (or **2**).

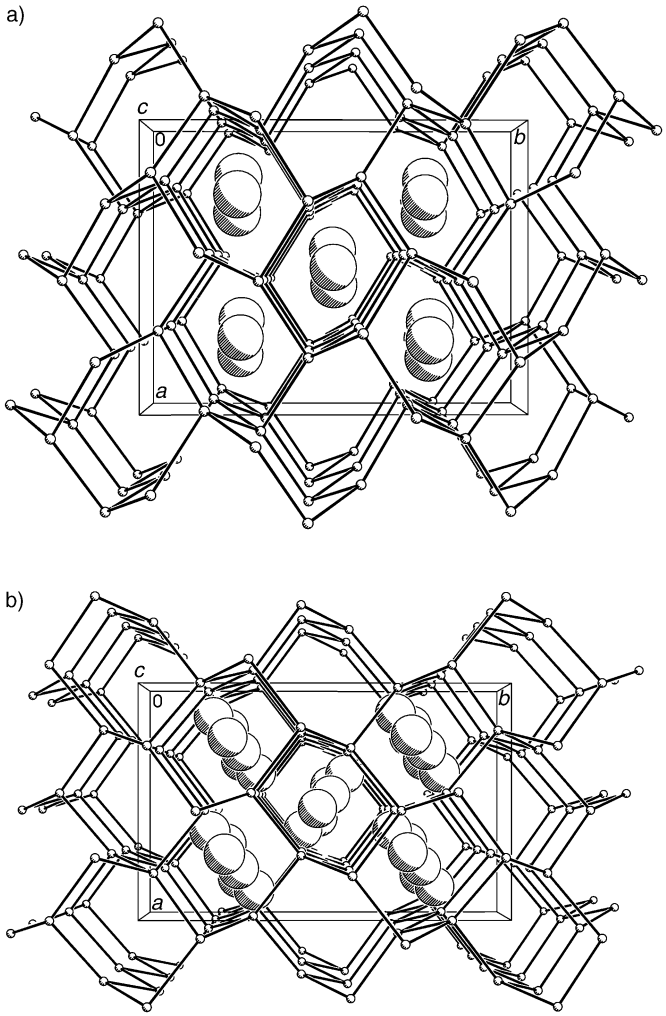

Figure 2. Ball-and-stick diagrams of the topological structure of **1** and **2**. Balls: cobalt(II) ions; sticks: imidazolate ligands; the space-filling molecules: pyridine in **1** and cyclohexanol in **2**.

*Crystal structure of compound **3***: Compound **3** has a 3D network (space group $I4_1$; noncentrosymmetric) that is identical to that reported thirty years ago.[9] This framework contains four crystallographically unique cobalt(II) ions (Co···Co 5.765–6.023 Å, N-Co-N angles 104.5–116.9°). In this framework, the SBUs are the 4-ring cobalt(II) rings which are doubly connected to wavelike or double crankshaft-like chains[16] (Figure 3a). These chains run along the *a* axis and intersect with those running along the *b* axis by means of the common 4-rings at the wave peaks to form an open 3D framework with a 12-ring opening (Figure 4a). Three such frameworks are interwoven and linked by the imidazolates at the cobalt(II) ions. As result, the 3D framework is again not the desired open framework. Nevertheless, the helical channels of $\approx 3.5 \times 3.5$ Å running along the *c* axis remain (the 8-rings in Figure 4b are such helical channels seen in projection), which, in principle, can host water molecules. Although there are no water molecules found in **3**, water molecules are found in $[Zn(im)_2]_\infty$ (**3′**),[17b] the isomorphous compound of **3**.

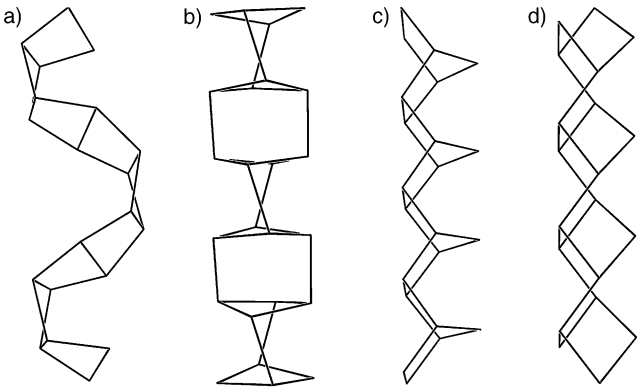

Figure 3. The structural subunits of cobalt imidazolate, which reveal the zeolitic nature of its structure. a) The double-crankshaft-like chain,[16] b) the Narsarsukite chain,[16] c) the A chain,[7] d) the B chain.[7]

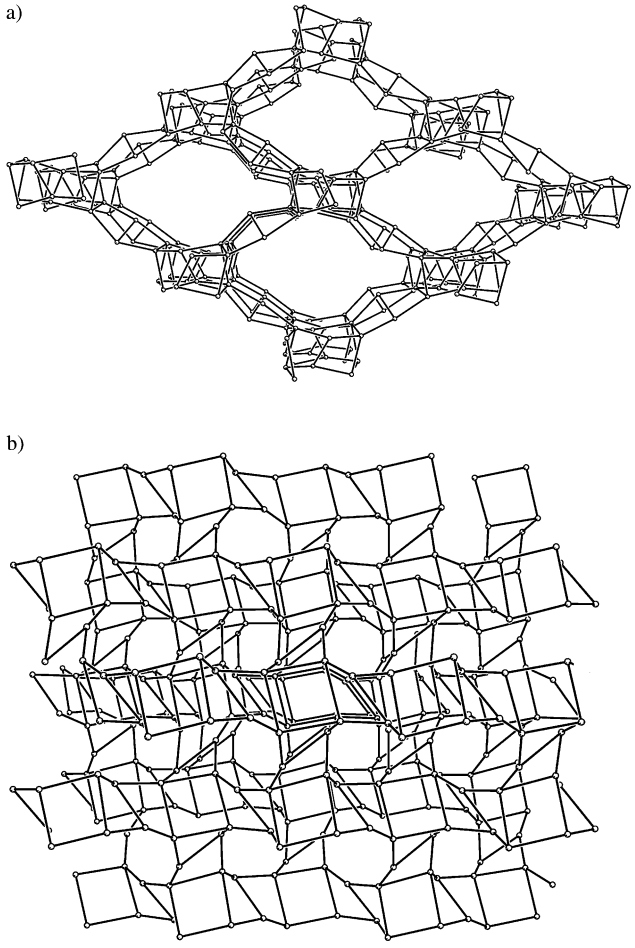

Figure 4. The open framework formed by the double-crankshaft-like chains in **3**. a) View along the *a* or *b* axis; c) view along the *c* axis.

*Crystal structure of compound **4***: Compound **4** is isomorphous with $[Zn(im)_2]_\infty$,[10] which was reported by Lehnert and co-workers 20 years ago. Similar to compound **3**, compound **4** also has a noncentrosymmetric 3D framework, but in this case the space group is $I4_1cd$ and it contains two crystallographically unique cobalt(II) ions (Co···Co 5.905–6.003 Å, N-Co-N angles 103.9–117.8°). This framework also

contains 4-rings which are connected to the Narsarsukite chain units[16] (Figure 3b). These chains run along the *c* axis parallel to each other within the C_4 symmetry and are linked to each other by the imidazolate ligands in *a* and *b* directions to give a 3D framework (Figure 5) by completing the 4-connections of the cobalt ions. This framework, according to reference [4], exhibits the network topology of banalsite with a pore opening of $\approx 4.0 \times 4.0$ Å.

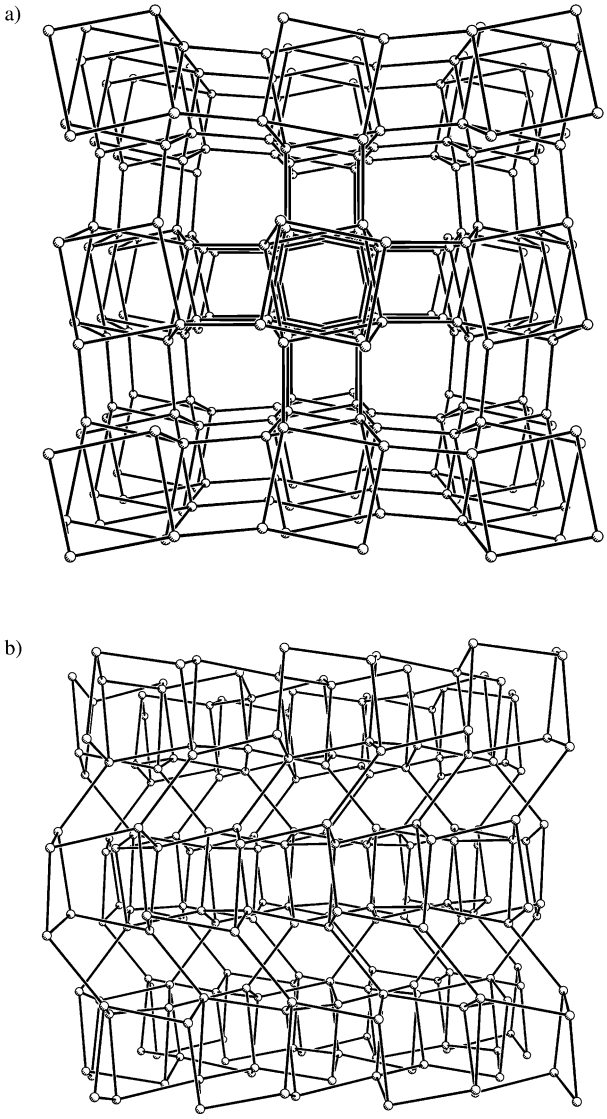

Figure 5. The 3D nets composed of Narsarsukite chains in **4**. a) View along the *c* axis; b) view along the *a* or *b* axis.

Crystal structure of compound ***5***: This compound exhibits a centrosymmetric open framework with zeolitic topology. In this framework, there are five crystallographically unique cobalt(II) ions, from which 4-, 5-, 6-, 7-, and 8-rings are generated. The Co···Co distance in framework **5** varies from 5.797 to 6.030 Å, and the N-Co-N angle varies from 104.0 to 118.8°. The structural subunits in the framework of **5** (Figure 6) are zeolite-like chain units A and B (Figure 3c, Figure 3d). Detailed descriptions of this structure can be found in reference [7].

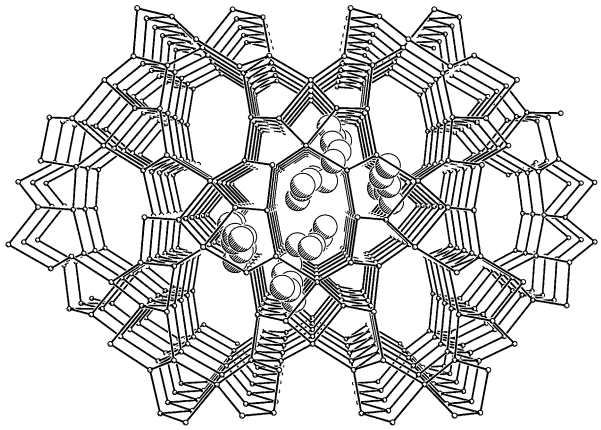

Figure 6. The 3D zeolitic net of **5** to highlight the open 1D channels along the *b* axis (the space-filling molecules are 3-methyl-1-butanol).

FTIR spectra: The IR spectra of all five compounds of cobalt imidazolate are distinguishable from each other, although the bands from their frameworks are almost completely coincident owing to the same IR signatures of the μ-imidazolate ligands (Table 3). Nevertheless, the IR spectra of the cobalt imidazolate frameworks can be classified into A and B types: type A has a single γ(C–H) band appearing in the range 751–758 cm^{-1}, while type B shows double γ(C–H) bands near 772 and 753 cm^{-1}. The IR spectra of **1, 2, 3**, and **5** fall under type A, which can be further distinguished from each other through the distinctive signatures of the guest molecules. In contrast, compound **4** appears to be the only polymorphous framework with type B IR signals, like all polymorphs of the reported copper(II) imidazolates.[4].

Thermal stability of the cobalt(II) imidazolate compounds: The thermal gravimetric analysis (TGA) of compound **1** shows complete desorption of the compound at about 230 °C. There is no further weight loss until 330 °C, and decomposition of the compound occurs at about 350 °C. Compound **2** loses its guest molecules completely at about 220 °C. There is no further weight loss until 430 °C, and decomposition of the compound is observed above 450 °C. The XRPD pattern of the pyridine-free matrix **1**, obtained by desolvation at 160 °C and 5×10^{-5} Torr vacuum for 3 h, shows that the lattice of the crystal has collapsed. However, the XRPD pattern of the cyclohexanol-free matrix **2**, obtained under the same conditions, shows that the crystalline periodicity remains unchanged so that another cyclohexanol-free motif **2′** can be obtained directly under solvatothermal conditions for which an X-ray single-crystal study has been undertaken.[17a] Compound **5** also has a stable porous framework structure. Details of the relevant studies have been reported in reference [7]. With relatively larger framework densities (Table 1), compounds **3** and **4** demonstrate almost the same TGA result: there is no weight loss until about 500 °C, above which the dramatic weight loss indicates decomposition of the compounds.

Table 3. IR spectroscopies for compounds **1**–**5**.

Frequencies [cm^{-1}]					
1	**2**	**3**	**4**	**5**	Assignments of the vibrational frequencies
	3584			3587	ν(O–H)
3130, 3107	3127, 3104	3129, 3106	3130, 3105	3129, 3104	ν(Ph–H)
	2926, 2853(d)			2956–2870(t)	ν(C–H)
1655–1577	1660–1589	1653–1566	1658–1596	1663–1597	ν(C–C)
1491, 1470	1489, 1468	1489, 1466	1489, 1467	1490, 1469	ring stretching of imidazolates
1435					ring stretching of pyridine
1317	1315	1315	1316	1316	δ(C–H)
1236	1235	1235	1233	1236	ring vibration
1165	1165	1164	1164	1166	ring breathing
1083	1084	1084	1081	1083	δ(C–H)
954, 846	953, 830	953, 826	952, 830	953, 831	ring bending
756	751	758	772, 753	755	γ(C–H)
706					γ(C–H) of pyridine
669	668	667	667	668	torsion

Magnetic properties of the cobalt(II) imidazolate polymers: Magnetic susceptibility of the crystalline samples **1**–**5** was measured at a field of 10 kOe from 2–300 K. The temperature dependence of the magnetic susceptibility in the high-temperature range ($T>30$ K), χ_M, can be fit to the Curie–Weiss expression, $\chi_M = C/(T-\theta)$, ($C = 0.125\, g^2S(S+1)$), with $g = 2.34$, $\theta = -26.4$ K for **1**; $g = 2.36$, $\theta = -26.2$ K for **2**; $g = 2.32$, $\theta = -31.2$ K for **3**; $g = 2.34$, $\theta = -32.4$ K for **4**; and $g = 2.31$, $\theta = -29.4$ K for **5**. These g values are all as expected for tetrahedral Co^{II} ions.[18a,d] At ≈300 K, the effective moments, $\mu_{eff} \equiv (8\chi T)^{1/2}$, are 4.4 (**1**), 4.3 (**2**), 4.1(**3**), 4.3 (**4**), and 4.3(**5**) μ_B, which are as expected for one high-spin tetrahedral Co^{II} ion with spin-orbit coupling.[18a,d] According to the obtained Weiss constants and the reciprocal molar magnetic susceptibilities from ≈300 to 2 K (Figure 7), a dominant weak antiferromagnetic coupling between the cobalt(II) ions in **1**–**5** can be suggested. However, in the low-temperature regions, the magnetic behaviors of the five compounds are quite different from each other (inset of Figure 7).

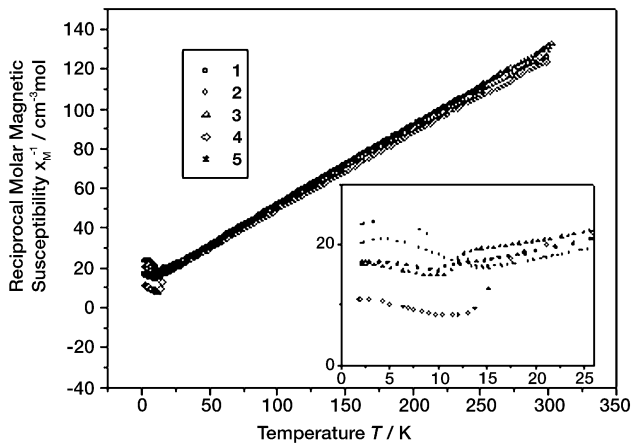

Figure 7. Reciprocal molar magnetic susceptibility χ^{-1} (M_t calculated with one Co^{II}) of **1**–**5** as functions of the temperature measured at 10 kOe field. Inset: the magnified plots in the low-temperature region show the different magnetic behaviors of the five compounds.

Compound ***1***: Figure 8a presents χ_M data versus T from 2 to 300 K and $d(\chi_M T)/dT$ data versus T obtained below 100 K. The results show that the magnetic susceptibilities increase from 0.01 cm^{3}mol^{-1} at 300 K to a maximum value of 0.062 cm^{3}mol^{-1} at ≈14.5 K, then, after a sharp downturn, they approach a value of 0.041 cm^{3}mol^{-1} by extrapolating the temperature to zero. This value accounts for about 2/3

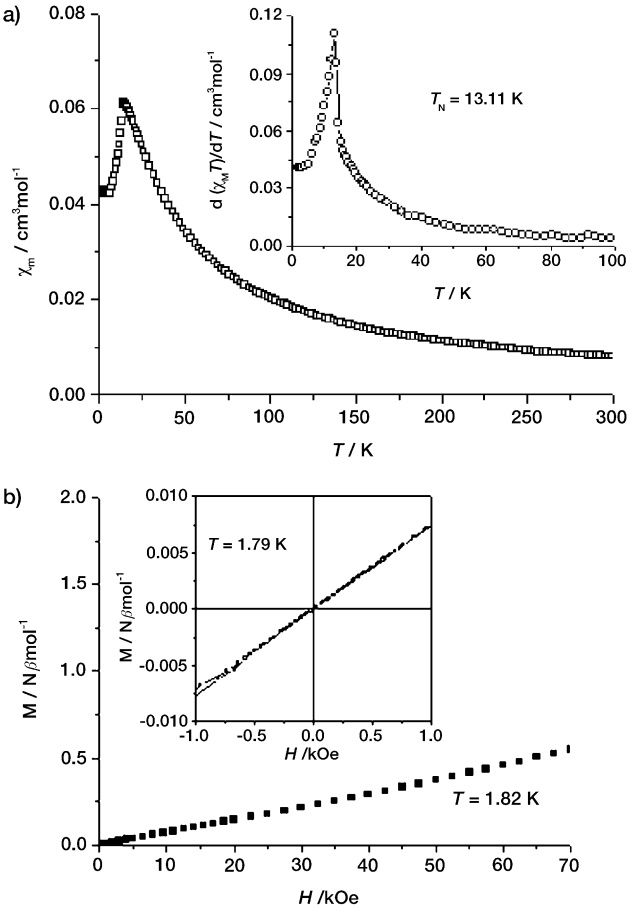

Figure 8. Plots of temperature dependence of χ_M and $d(\chi_M T)/dT$ of **1** measured at 10 kOe field. b) Magnetization versus applied magnetic field at 1.82 K and field dependence of magnetization cycling at 1.79 K for **1**.

of the maximum χ_M value of 0.062 $cm^3 mol^{-1}$, the typical character of an antiferromagnet. The $d(\chi_M T)/dT$ versus T curve shows a maximum value at 13.11 K for the Neel temperature (T_N).[19] According to these results, antiferromagnetic coupling between the cobalt(II) ions with an antiferromagnetic ordering below 13.11 K is suggested. This is also supported by the magnetization values below T_N which vary linearly with the applied fields up to the maximum field strength studied (70 kOe); no net magnetization was observed at an applied field of zero. Further evidence for **1** to be an antiferromagnet comes from the reversible lines through the center observed upon cycling the field between +10 and −10 kOe at 1.82 K (Figure 8b).

Compound ***2***: Susceptibility χ_M versus T from 2 to 300 K and $d(\chi_M T)/dT$ versus T below 100 K plots are shown in Figure 9a. Similar to compound **1**, the susceptibility increases from 0.01 $cm^3 mol^{-1}$ at ≈300 K to a maximum value of 0.063 $cm^3 mol^{-1}$ near 15 K, then, decreases sharply to a value of 0.045 $cm^3 mol^{-1}$, the extrapolated value at zero temperature. However, this value cannot be fitted to the 2/3 relationship with the maximum susceptibility as is the case for compound **1**. From the temperature dependence of $d(\chi_M T)/dT$, the maximum value of $d(\chi_M T)/dT$ was acquired and the antiferromagnetic ordering below 13.5 K (T_N) was indicated. However, the low-field field-cooled (FC) temperature dependence of magnetization acquired while cooling from 20 K in an applied field of 200 Oe (Figure 9b) reveals a ferromagnetic phase transition related to spin canting below 15 K (T_C). Hysteretic behavior (with a visible loop) was observed at 1.82 K and the magnetization at this temperature in the applied field to the maximum strength of 70 kOe increases, as in compound **1**, almost linearly and slowly with the applied field; however, very small net magnetization is observed at zero field (Figure 9d). All of this is evidence of a very weak ferromagnetism caused by small, uncompensated antiferromagnetic spin-canting. With regards to **2** being a ferromagnet, further evidence comes from the AC susceptibility (Figure 9c): in different applied AC field frequencies, the χ_{AC} responses are frequency independent and they appear in both the in-phase χ' and out-of-phase χ'' reflections at about 15 K.

Compound ***3***: Magnetic susceptibility χ_M and $\chi_M T$ versus temperature plots are shown in Figure 10a. As the temperature is lowed from 300 K, the value of $\chi_M T$ decreases. The

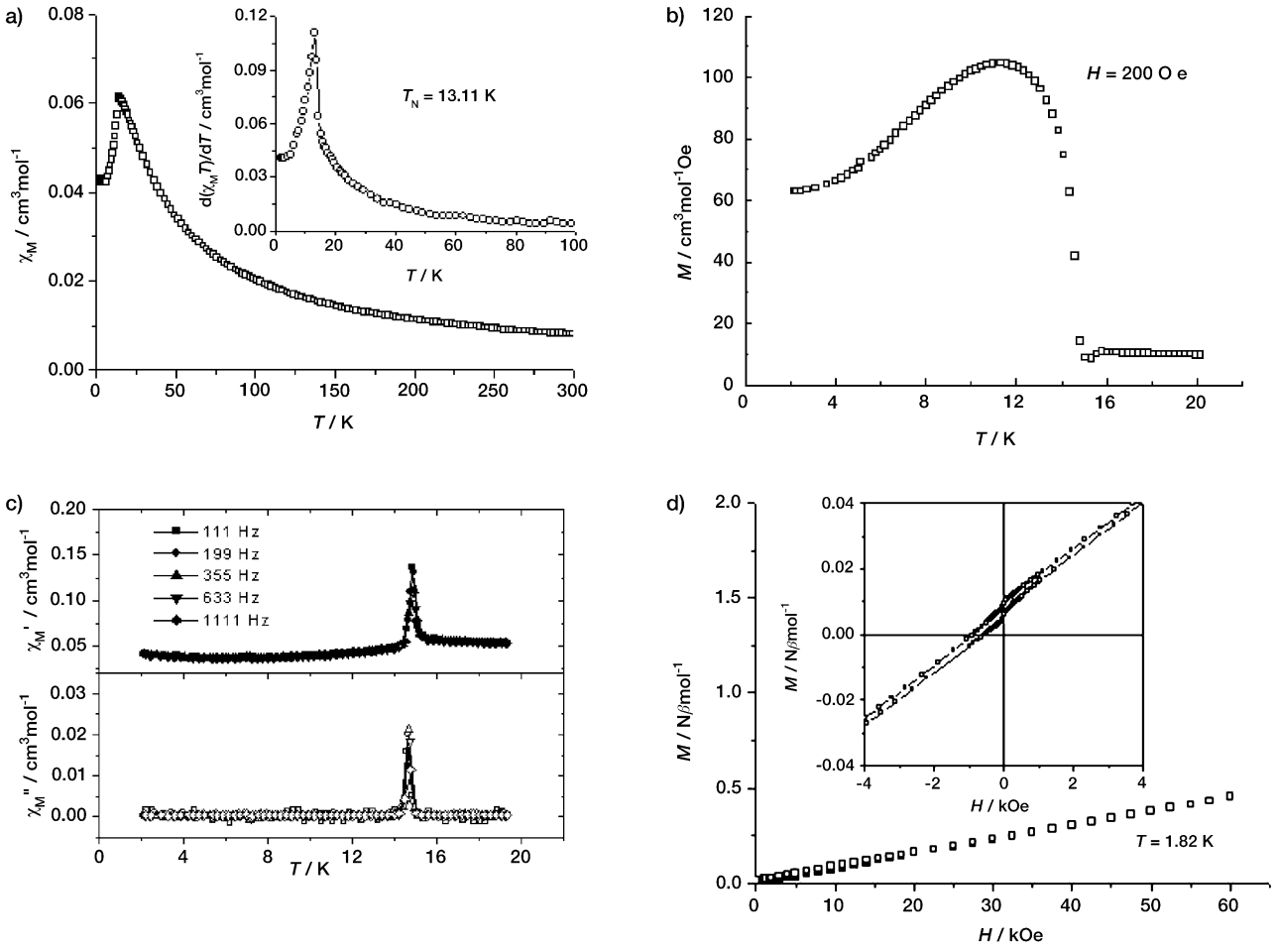

Figure 9. a) Plots of temperature dependence of χ_M and $d(\chi_M T)/dT$ for **2** measured at 10 kOe field. b) Plot of field-cooled (FCM) for **2** at 200 Oe field. c) Plots of temperature dependence of AC susceptibility χ'(top) and χ''(bottom) obtained at 0.1 Oe field for **2**. d) Magnetization versus applied magnetic field at 1.82 K and hysteresis loop in the ±4 kOe range at 1.82 K for **2**.

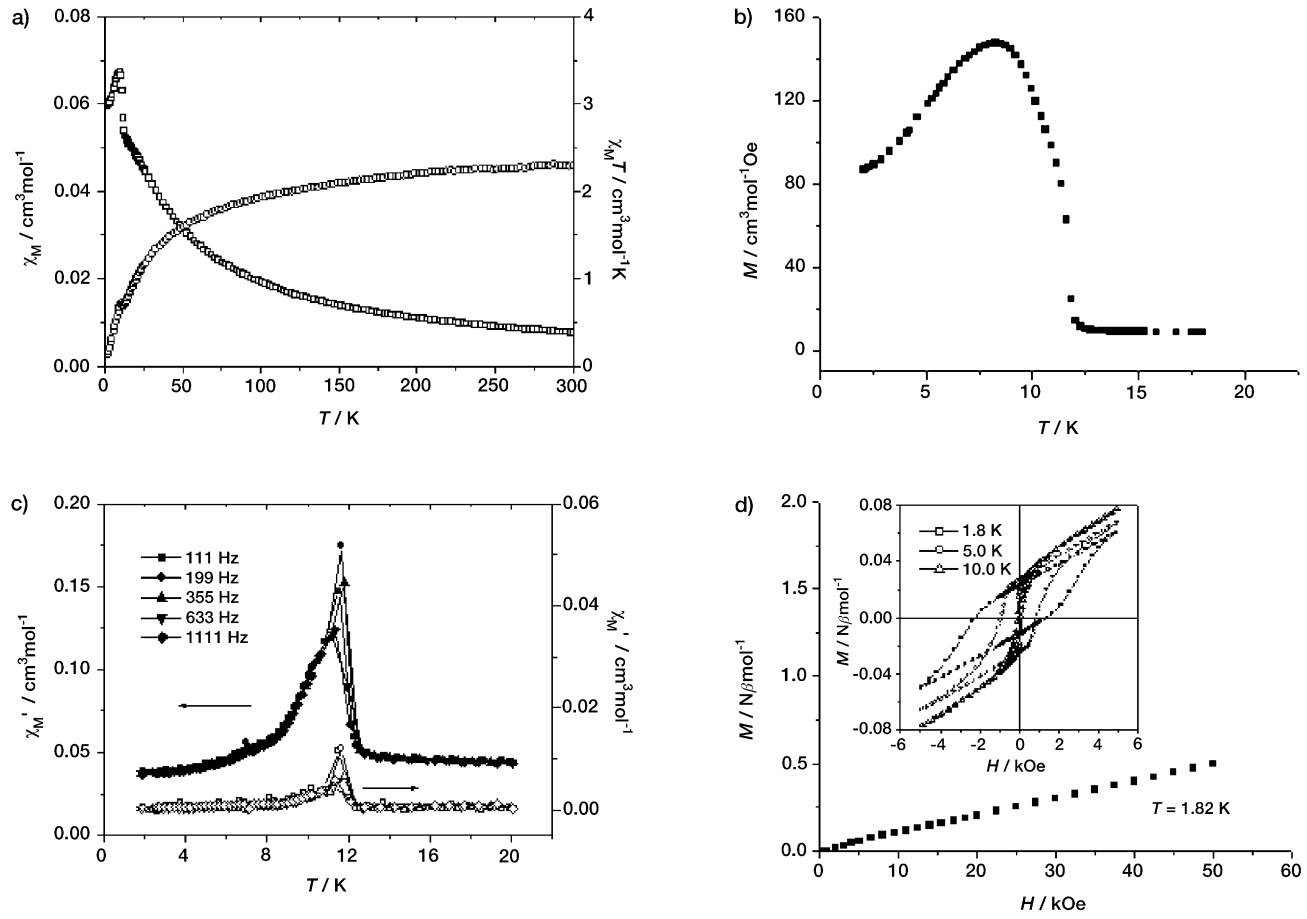

Figure 10. a) Plots of temperature dependence of χ_M (left) and $\chi_M T$ (right) for **3** measured at 10 kOe field. b) Plots of field-cooled (FCM) measured at 200 Oe field for **3**. c) Plots of temperature dependence of AC susceptibility χ'(top) and χ''(bottom) obtained at 50 Oe field for **3**. d) Magnetization versus applied magnetic field at 1.82 K and hysteresis loops in the ± 6 kOe range at 1.8, 5.0, and 10.0 K for **3**.

minimum value of $\chi_M T$ occurs before a small abrupt increase at $\approx$11.5 K, after which the value of $\chi_M T$ decreases linearly to 2 K. The magnetic transition at 11.5 K is indicative of the onset of a ferromagnetic ordering resulting from spin-canted antiferromagnetic coupling. Support for such a ferromagnetic ordering comes from the low-field field-cooled (FC) magnetization (Figure 10b). The plot of M versus T at an applied field 200 Oe in the temperature range 2–20 K shows that an abrupt increase of the M value occurs at 11.5 K, which indicates a ferromagnetic phase transition. Further support comes from cycling the applied field between $+5$ and -5 kOe at 1.8, 5, and 10 K, which have generated hysteresis loops (Figure 10d). From these loops, the coercive fields of 1800, 1000, and 10 Oe are observed and remnant magnetizations of 0.016, 0.023, and 0.017 N$\mu_B$mol^{-1} are obtained at 1.8, 5, and 10 K, respectively. Magnetization versus applied field at 1.8 K demonstrates in Figure 10d that it varies linearly from 7 up to 50 kOe, and reaches a magnetization value of 0.5 Nβmol^{-1} at 50 kOe, significantly below the theoretical saturation value of 3 Nβ [for $g = 2$, high-spin tetrahedral coordinated Co^{II} ($s = 3/2$)] suggesting a long-range ferromagnetic ordering resulting from the spin-canted antiferromagnetic coupling.

To confirm the magnetic ordering, the temperature dependencies of the in-phase, $\chi'(T)$, and out-of-phase, $\chi''(T)$ components of the AC susceptibility were measured (Figure 10c). In different applied AC field frequencies, the χ_{AC} responses are frequency independent and an out-of-phase reflection χ'' appears at 11.5 K, which is further evidence of long-range ferromagnetic ordering.

Compound ***4***: Magnetic susceptibility χ_M and $\chi_M T$ versus temperature data are shown in Figure 11a. As the temperature decreases from $\approx$300 K, the $\chi_M T$ value decreases gradually. At $\approx$15.5 K, the $\chi_M T$ value increases abruptly, reaching a maximum at $\approx$15 K before decreasing rapidly on further cooling to 2 K. This behavior suggests antiferromagnetic coupling between cobalt(II) centers and a ferromagnetic magnetic ordering below the 15 K (T_C). Support for the ferromagnetic ordering comes from the low-field FC magnetization (Figure 11b) showing the onset below 15.5 K. Further evidence that confirms the magnetic ordering below 15.5 K is provided by the temperature dependencies of *$\chi'(T)$ and $\chi''(T)$* (Figure 11c), both of which have strong responses independent of the AC field frequency. The critical temperature (T_C) of 15.5 K indicative of the bulk magnetic ordering is determined according to the peak position of χ' at 111 Hz.

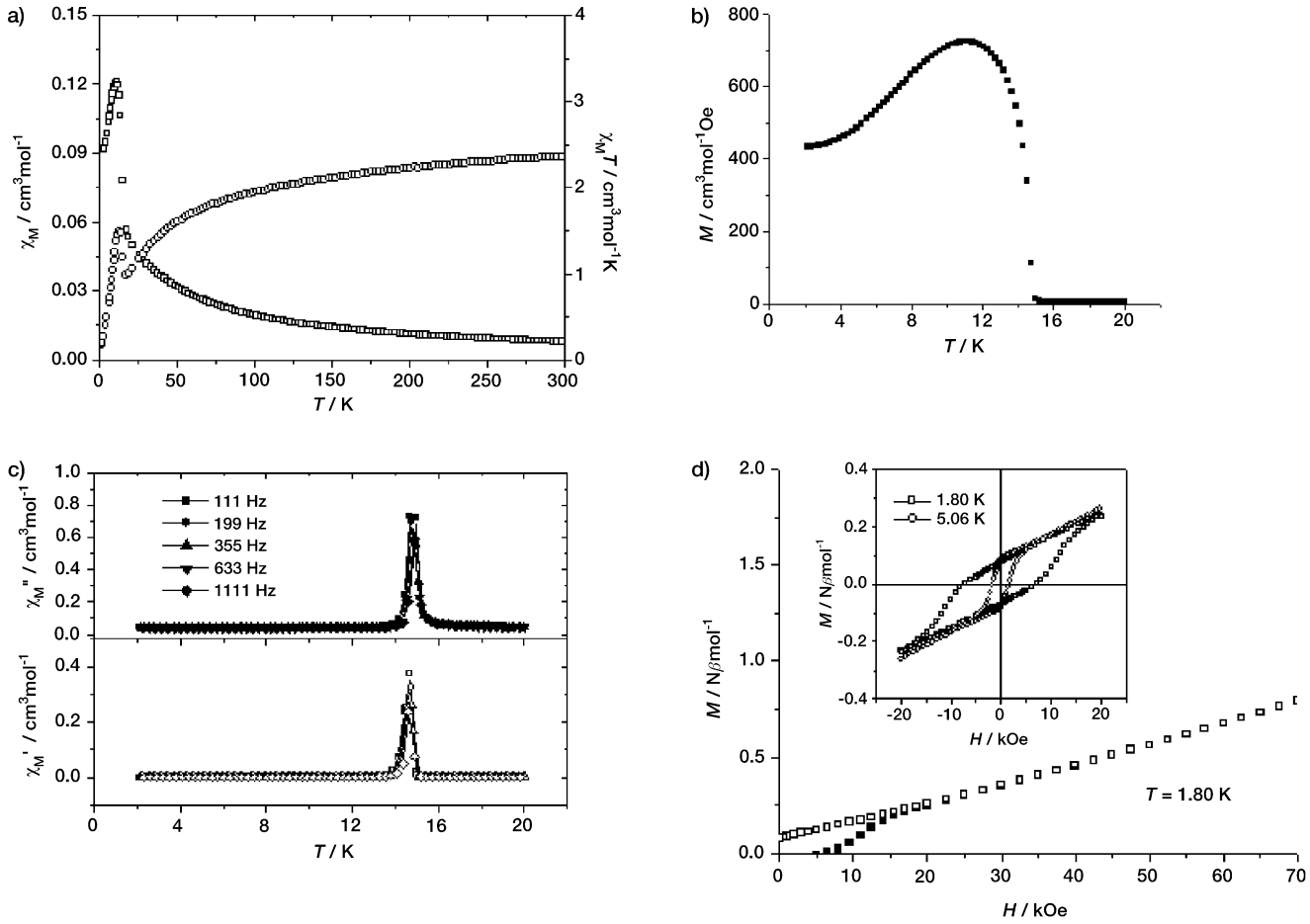

Figure 11. a) Plots of temperature dependence of χ_M (left) and $\chi_M T$ (right) for **4** measured at 10 kOe field. b) Plot of field-cooled (FCM) measured at 200 Oe field for **4**. c) Plots of temperature dependence of AC susceptibility χ'(top) and χ''(bottom) obtained at 20 Oe field for **4**. d) Magnetization versus applied magnetic field at 1.8 K and hysteresis loops in the $\pm$20 kOe range at 1.8 and 5.0 K for **4**.

The magnetic hysteresis (Figure 11 d) at 2 and 5 K between $\pm$20 kOe shows a coercive field of 7300 and 1700 Oe with small remnant magnetization of 0.07 and 0.09 Nβmol^{-1}, respectively. At 1 K, the magnetization (Figure 11 d) above 15 kOe varies almost linearly as the applied field increases and reaches 0.7 Nβmol^{-1} at 70 kOe, which is also significantly below the predicted saturation value of 3 Nβmol^{-1}.

Compound ***5***: Magnetic behavior of **5** at high temperatures is almost as same as that of the other four compounds according to the plot of $\chi_M T$ versus temperature (Figure 12 a). However, in the low-temperature range, the magnetic behavior is quite different: in the low-field FC magnetization M versus T at applied field 200 Oe in the temperature range 2–20 K (Figure 12 b), although the magnetic phase transition arising from spin-canting is observed at 10.3 K and, furthermore, the hysteresis loops at 1.8 and 5.0 K (Figure 12 d) are also presented. However, the result of the AC susceptibility reveals that compound **5** can be regarded as a hidden spin-canted antiferromagnet because the obvious in-phase $\chi'(T)$ cusps appear at 10.6 K and they are frequency independent while the corresponding $\chi''(T)$ components are not observed.[20]

Discussion

The extended polymorphism of cobalt(ii) imidazolate (or copper(ii) imidazolate) 3D frameworks is a rare phenomenon in polymeric coordination compounds, although polymorphism is more general than expected in some polymeric systems.[14,21] However, for the polymeric coordination compounds that maintain an identical framework composition and coordinate style, to give at least five different topological framework structures, this phenomenon must arise from some inherent structural features of the compounds and we attribute this, in the case of cobalt(ii) imidazolates (or copper imidazolates) to the special conformational flexibility of zeolite-like structures that results from the special coordinate orientations of the imidazolate ligand. The rotation of imidazolate about the Co–N bonds affords a wider range of Co-Co-Co (T-T-T) angles than those of the corresponding linear ligand, such as 4,4′-bipyridine,[22] in which the T-T-T angles are not greatly different from the N-T-N angles. This makes the cobalt(ii) imidazolate more facilitate the formation of the smaller or larger T-atom rings and benefits generating the structures of zeolitic topology. For example, there are 4-, 5-, 6-, 7-, and 8-rings in the framework of **5**, in which the Co-Co-Co angles vary from 74.8 to 163.2°, while the N-

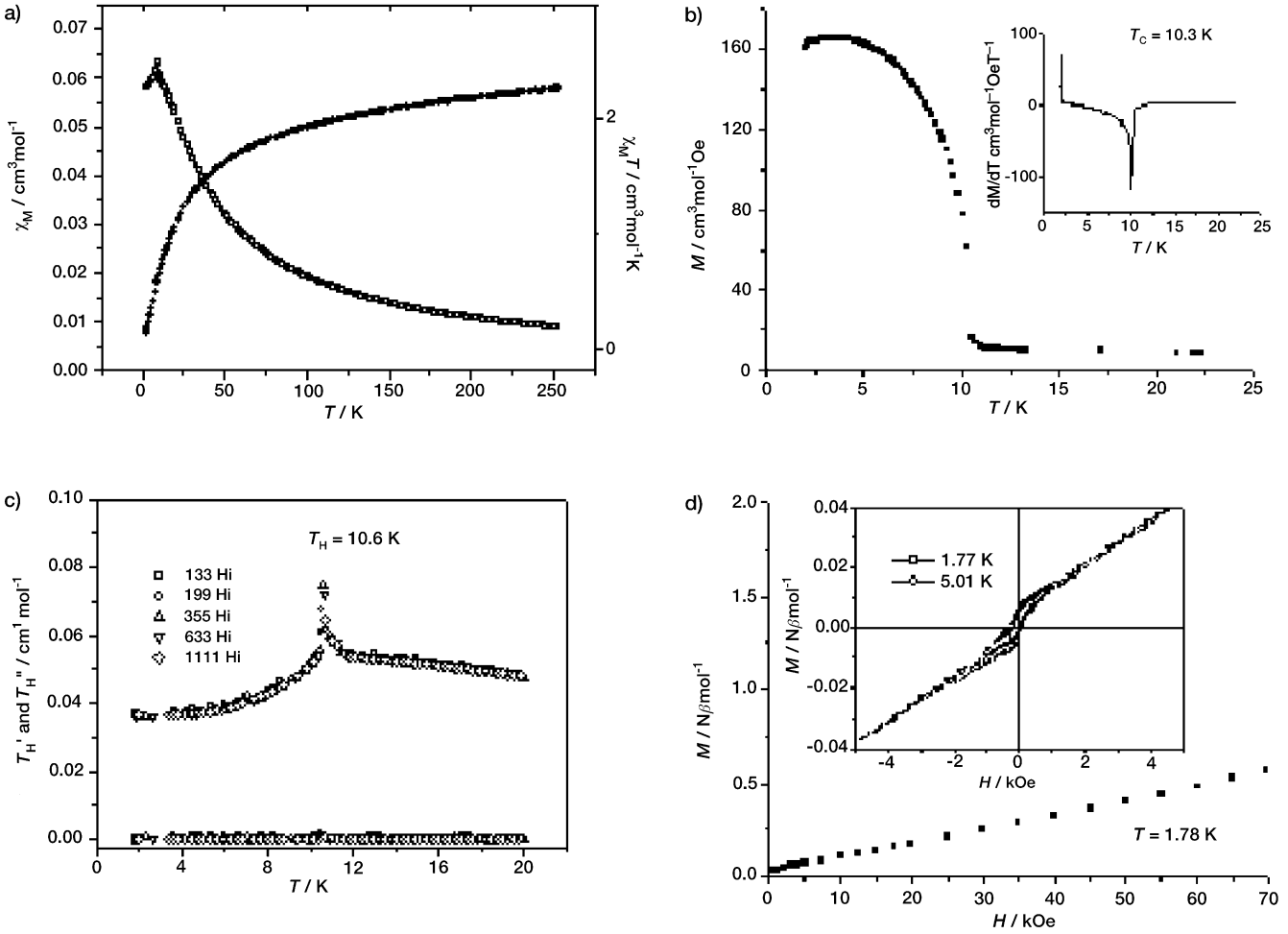

Figure 12. a) Plots of temperature dependence of χ_M (left) and $\chi_M T$ (right) for **5** measured at 10 kOe field. b) Plot of field-cooled (FCM) measured at 200 Oe field for **5**. c) Plots of temperature dependence of AC susceptibility χ'(top) and χ''(bottom) obtained at 2 Oe field for **5**. d) Magnetization versus applied magnetic field at 1.78 K and hysteresis loops in the $\pm$50 kOe range at 1.77 and 5.01 K for **5**.

Co-N angles vary from 104.0 to 118.8°, which shows relative minimal differences from those of the other four compounds of cobalt imidazolate (Table 4). These rings that have generated more than a hundred different structures of zeolites or zeolite-like molecular sieves. Therefore, it is reasonable to compare the cobalt(II) imidazolates to the silicalite or zeolite together and we predict that there are even more polymorphous frameworks of cobalt imidazolate to be explored. Nevertheless, the compounds of cobalt(II) imidazolate reported herein are only obtained with the silica-like metal–organic frameworks, of which the polymorphs **3** and **4** are related to the dense phases of silica with formula [M(im)$_2$] (corresponding to the dense silica SiO_2) and the polymorphous frameworks of **1, 2**, and **5** are related to the porous phases of silica with the formula [M(im)$_2$·xG] (corresponding to the porous silica, the silicalite [SiO_2·xG] (G = guest molecule)). Although we have managed to form hybrids between the cobalt imidazolate and M^{III} T atoms or O atoms, the reasons for the lack of success may lie the synthetic strategy. We assume that if a rationale synthetic strategy could be developed, the zeolite-like or $AlPO_4$-like structures of metal imidazolate might be realizable and the polymorphism of cobalt imidazolate or metal imidazolate frameworks could then be greatly extended.

Table 4. Geometrical parameters of the five cobalt(II) imidazolate compounds

	1	**2**	**3**	**4**	**5**
Co–N[(Å]	1.968, 2.013	1.987, 2.007	1.954–2.013	1.938–2.054	1.966–2.008
Co···Co[Å]	5.855, 5.945	5.860, 6.032	5.765–6.023	5.905–6.003	5.797–6.030
N-Co-N[°]	102.7–112.8	105.5–113.2	104.5–116.9	103.9–117.8	104.0–118.8
Co···Co···Co[°]	74.9–142.4	83.9–141.7	67.3–161.3	81.6–138.9	74.8–163.2
circuits	6	6	4	4, 6	4, 5, 6, 7, 8
SBUs	6^6 cage	6^6 cage	4-ring chain	5-, 6-ring chain	chain A, B
net topology	3D (6,4-net)	3D (6,4-net)	3D tetranodal	3D banalsite	3D zeolite-like

Like in the synthesis of zeolite, there are also many variables (the structure-directing agents, template agents, solvents, and temperature as well as the amount of the used solvent) that can be adjusted in the syntheses of cobalt imidazolates. Changing these variables may lead to the generation of different polymorphous frameworks of cobalt(II) imidazolate (Table 1). First, the porous frameworks of cobalt imidazolate like those of silicalites are kinetically controlled, while the dense frameworks are controlled thermodynamically. To create such materials with even larger pores, a new synthetic strategy at low temperature is required and our efforts in this regard are ongoing. Second, although the mechanism for solvatothermal synthesis of cobalt(II) imidazolate is not yet clear, we are certain that the mechanism here is different from that in a zeolite synthesis. The structure-directing agents play an important role in generating the porous species of cobalt imidazolate (Table 1); these agents may have served not only as the bases to deprotonate the imidazole, but also as coordinate ligands to form the intermediary coordination compounds, which are then translated into the final crystalline products under solvatothermal conditions. The experiments also revealed that the trialkylamines commonly used in zeolite synthesis are not as capable of directing the cobalt(II) imidazolate to a crystalline substance since they cannot serve as ligands. It also seems that piperazine is an effective structure-directing agent, although the mechanism is not yet clear. Up to now, only a limited number of structure-directing agents and solvents (template agents) have been tested. Therefore, the elucidation of the structure-directing effects and the optimization of the conditions will require much futher study.

With regard to the magnetic properties, the imidazolate linkages of compounds **1**–**5** transmit the antiferromagnetic interactions between the cobalt(II) ions, and the magnetic behavior of the compounds resembles the common characters of tetrahedrally coordinated cobalt:

1) Compared to compounds of tetrahedral cobalt(II) with magnetic ordering temperatures below 1 K[18b] which are associated with weak magnetic exchange between the cobalt ions, compounds **1**–**5** exhibit higher magnetic ordering temperatures that may be attributed to relatively strong magnetic interactions between the cobalt ions that are transmitted by the imidazolate bridges rather than to the single ion anisotropy of Co^{II}.[23] According to the θ values of compounds **1**–**5** and the conventional mean-field expression for a Heisenberg antiferromagnet,[24] $J/k_b = 3\theta/[2zS(S+1)]$, where $z = 4$ is the number of nearest neighbors, the values of J/k_b are estimated to be −2.6 K for **1** and **2**, −3.1 K for **3**, −3.2 K for **4**, and −2.9 K for **5**, respectively. They are thus approximately two times greater than that in β-$Co^{II}[N(CN)_2]_2$.[25]
2) According to the g values of compounds **1**–**5** in the range 2.2–2.4, which were obtained by fitting the Curie–Weiss expression, $\chi_M = 1/(T-\theta)$, the small anisotropic g values are characterized as typical tetrahedral cobalt ions ordered in $s = 3/2$ spin with small zero-field splitting.
3) The weak magnetism in **2**–**5** arises from the spin canting of the antiferromagnetically interacted Co^{II} ions. The origin of the spin canting should be mainly due to the antisymmetric interaction between the neighboring Co^{II} ions, in combination with possible local anisotropy of Co^{II} ions. For all five compounds reported here, single-bridging imidazolate linkages between Co^{II} ions produce low-symmetry Co^{II}-L-Co^{II} exchange pathways, which should be responsible for the antisymmetric interactions, even though the space group of **5** is centrosymmetric. On the other hand, the weak ferromagnetism from canting may be hidden when many sublattices are present, such as in the case of **5**.[18c,20] Why compounds **1** and **2** have such different magnetic behaviors, is still an open question.

Conclusion

The work reported here focuses on the synthesis of open metal–organic frameworks with zeolitic topologies. Considering the structural motif of zeolites, we devised the metal-organic building block $[Co(im)_4]^{2-}$, from which the silica-like structures of extended polymorphous frameworks of cobalt(II) imidazolate have been realized by a modification of a strategy to synthesize zeolites. Superior to gas-phase synthesis,[9b,10] the solvatothermal method favors not only the generation of crystalline products that are suitable for X-ray single-crystal analysis, but also of porous structures if the proper structure-directing agents and templates (or space-filling agent) are employed. More interestingly, the polymorphous frameworks contain structural features reminiscent of those in silica. Although up to now the polymorphous frameworks of cobalt(II) imidazolate with cristobalite-, tridymite-, or quartz-like structures have not yet been obtained, we believe that they exist because we recently obtained a cadmium imidazolate $[Cd(im)_2]_\infty$[26] with a twofold interpenetrated cristobalite-like structure. Moreover, the different structures of cobalt(II) imidazolates have indeed afforded various magnetic behaviors that are theoretically significant for the understanding of the relationship between structures and magnetic properties and further for a rational design of molecular magnetic materials.

Experimental Section

General procedure: All chemicals and solvents used in the syntheses were from commercial sources and used without further purification except for the piperazine hexahydrate (PZ) which was treated at 140 °C under 10 mmHg vacuum for 2 h and was used arbitrarily as piperazine dihydrate in the syntheses.

Physical measurements: Elemental analysis for C, H, and N were carried out at the Materials Analysis Center of Nanjing University with a Perkin-Elmer 240 analyzer. Fourier-transform IR (FT-IR) Spectra were recorded in KBr pellets on a Nicolet FT-IR 17SX. Thermogravimetric analyses (TGA) were carried out with a TA-SDT 2960 and a heating rate of 5 °C min^{-1} from 20–600 °C under a flux of nitrogen.

Magnetic measurements: The magnetic measurements for **1**–**5** were carried out on crystalline samples with a MagLab System 2000 magnetometer in a magnetic field up to 70 KOe. Diamagnetic corrections were estimated from Pascal's constants.

$[Co_2(im)_4$ñPy$]_8$ (1): $Co(Ac)_2{\cdot}4H_2O$ (1.245 g, 5.0 mmol) was dissolved in pyridine (15 mL) and a solution of imidazole (10 mmol) in 3-methyl-1-butanol (MB, 15 mL) was added. The mixture was stirred at room temperature for 12 h to give a heterogeneous violet mixture which was then placed into a Teflon-lined autoclave (34 mL). The autoclave was sealed and heated at 140 °C for 24 h. After the mixture was cooled to room temperature, violet crystals were collected and washed with ethanol (3× 15 mL; yield: 80%). Elemental analysis calcd (%) for $C_{17}H_{17}N_9Co_2$ ($[Co_2(im)_4{\cdot}Py]_8$): C 43.88, H 3.68, N 27.10; found: C 43.64, H 3.71, N 26.68.

$[Co_2(im)_4$ñCyhol$]_8$ (2): $Co(Ac)_2{\cdot}4H_2O$ (1.245 g, 5.0 mmol) was dissolved in cyclohexanol (10 mL) and then a cyclohexanol solution (20 mL containing 10 mmol imidazole and 5 mmol piperazine) was added. The heterogeneous mixture was stirred at room temperature for 12 h and then was placed into a Teflon-lined autoclave (34 mL). The autoclave was sealed and heated at 140 °C for 24 h. After the mixture was cooled to room temperature, violet crystals were collected and washed with ethanol (3× 15 mL; yield: 85%). Elemental analysis calcd (%) for $C_{18}H_{24}N_8OCo_2$ ($Co_2(im)_4{\cdot}Ch]_8$): C 44.45, H 4.97, N 23.05; found: C 44.31, H 4.65, N 22.64.

$[Co_2(im)_4$ñ0.25$H_2O]_8$ (2′): Following the procedure for the preparation of compound **2**, cyclohexanol was replaced with *tert*-butyl alcohol to afford violet crystals formulated as $C_{12}H_{12.5}N_8O_{0.25}Co_2$ in a very poor yield. X-ray single-crystal analysis showed that this is the cyclohexanol-free analogue[17a] of **2**.

$[Co(im)_2]_8$ (3): Following the procedure for preparation **1**, MB was replaced by ethanol. Violet crystals of **3** were obtained (yield: 78%). Elemental analysis calcd (%) for $C_6H_6N_4Co$ ($Co(im)_2]_8$): C 37.32, H 3.13, N 29.02; found C 37.56, H 3.36, N 28.85. An isomorphous compound of **3**, the zinc analogue,[17b] was also prepared by means of the same procedure. Elemental analysis calcd (%) for $C_6H_7N_4O_{0.25}Zn$ ($[Zn(im)_2{\cdot}0.25H_2O]_8$ (**3′**)): C 35.33, H 3.19, N 27.46; found: C 35.65, H 2.85, N 27.81.

$[Co(im)_2]_8$ (4): Following the procedure for the preparation of polymorph **1**, pyridine was replaced by quinoline. Violet crystals formulated as $C_6H_6N_4Co$ were obtained (yield: 60%). Elemental analysis calcd (%) for $C_6H_6N_4Co$ ($[Co(im)_2]_8$): C 37.32, H 3.13, N 29.02; found: C 37.41, H 3.34, N 28.71.

$[Co_5(im)_{10}{\cdot}2MB]_8$ (5): Compound **5** was prepared according to the procedure given in our recently published work.[7]

X-ray single-crystal structure determination: Crystallographic measurements (except for compound **5**) were carried out on a Enraf Nonius-CAD4SDP44 diffractometer with graphite-monochromated $Mo_{K\alpha}$ radiation (λ = 0.71073 Å), and unit cell parameters were based on 25 carefully centered reflections in the range $4.42 < 2\theta < 51.96°$. Absorption correction was applied by means of ψ scan data. The structures were solved by direct methods and refined by full-matrix least-squares on F^2 values with SHELXS-97 (version 5.1) package of crystallographic software.[27] All non-hydrogen atoms (sometimes excluding those of solvent molecules) were refined anisotropically. Hydrogen atoms were generated and included in the structure factor calculations with assigned isotropic thermal parameters but were not refined. For the full-matrix least-squares refinements [$I > 2\sigma(I)$], the unweighted and weighted agreement factors of $R = \Sigma(||Fo| - |Fc||)/\Sigma|Fo|$ and $wR = \{\Sigma w[(F_o^2 - F_c^2)^2]/\Sigma w[(F_o^2)^2]\}^{1/2}$ ($w = 1/[\sigma^2(F_o^2) + (aP)^2 + bP]$, where $P = (F_o^2 + 2F_c^2)/3$) were used. In the noncentrosymmetric space groups, the Flack parameter defined as $|F| = (1-x)|F(+)| + x|F(-)|$ was refined to determine the absolute configuration.[28] Crystal data and detail of the structure determinations for **1**–**5** are summarized in Table 2.

CCDC-149555 (**1**), CCDC-212355 (**2**), CCDC-212356 (**2′**), CCDC-212357 (**3′**), CCDC-212358 (**4**) and CCDC-168798 (**5**) contain the supplementary crystallographic data for this paper. These data can be obtained free of charge via www.ccdc.cam.ac.uk/conts/retrieving.html (or from the Cambridge Crystallographic Data Centre, 12 Union Road, Cambridge CB2 1EZ, UK; fax: (+44) 1223-336033; or deposit@ccdc.cam.uk).

Acknowledgment

This work was supported by the State Key Project of Fundamental Research (No. G200077500, G1998061305) and the Natural Science Foundation of China (No. 90101028 and 20221101). S.G. acknowledges the National Science Fund for Distinguished Young Scholars (No. 20125104).

[1] a) C. Janiak, *Angew. Chem.* **1997**, *109*, 1499–1502; *Angew. Chem. Int. Ed. Engl.* **1997**, *36*, 1431–1434; b) P. J. Hagrman; D. Hagrman; J. Zubieta, *Angew. Chem.* **1999**, *111*, 2798–2848; *Angew. Chem. Int. Ed.* **1999**, *38*, 2638–2684; c) A. K. Cheetham, G. Férey, T. Loiseau, *Angew. Chem.* **1999**, *111*, 3466–3492; *Angew. Chem. Int. Ed.* **1999**, *38*, 3268–3292.

[2] S. R. Batten, R. Robson, *Angew. Chem.* **1998**, *110*, 1558–1595; *Angew. Chem. Int. Ed.* **1998**, *37*, 1460–1494.

[3] a) S. S.-Y. Chui, S. M.-F. Lo, J. P. H. Charmant, A. G. Orpen, I. D. Williams, *Science*, **1999**, *283*, 1148–1150; b) H. Li, M. Eddaoudi, M. O'Keeffe, O. M. Yaghi, *Nature*, **1999**, *402*, 276–279; c) M. Eddiaoudi, D. B. Moler, H. Li, B. L. Chen, T. M. Reineke, M. O'Keeffe, O. M. Yaghi, *Acc. Chem. Res.* **2001**, *34*, 319–330.

[4] N. Masciocchi, S. Bruni, E. Cariati, F. Cariati, S. Galli, A. Sironi, *Inorg. Chem.* **2001**, *40*, 5897–5905, and references therein.

[5] N. Masciocchi, A. Sironi, *J. Chem. Soc. Dalton Trans.* **1997**, 4643–4650.

[6] a) P. K. Coughlin, S. J. Lippard, *Inorg. Chem.* **1984**, *23*, 1446–1451; b) K. Matsumoto, S. Ooi, Y. Nakao, W. Mori, A. Nakahara, *J. Chem. Soc. Dalton Trans.* **1981**, 2045–2048; c) P. Chaudhuri, I. Parpenstein, M. Winter, M. Lengen, C. Butzlaff, E. Bill, A. X. Trautwein, U. Flörke, H.-J. Haupt, *Inorg. Chem.* **1993**, *32*, 888–894; d) P. Chaudhuri, I. Parpenstein, M. Winter, C. Butzlaff, E. Bill, A. X. Trautwein, U. Flörke, H.-J. Haupt, *Inorg. Chem.* **1992**, 321–322; e) J. P. Costes, M. I. Fernandez-Garcia, *Inorg. Chim. Acta* **1990**, *173*, 247–254; f) H. Ohtsu, I. Shinobu, S. Nagatomo, T. Kitagawa, S. Ogo, Y. Watanabe, S. Fukuzumi, *Chem. Commun.* **2000**, 1051; g) Z.-W. Mao, D. Chen, W.-X. Tang, K.-B. Yu, L. Liu, *Polyhedron*, **1992**, *11*, 191–196.

[7] Y.-Q. Yian, C.-X. Cai, J. Ji, X.-Z. You, S.-M. Peng, G.-H. Lee, *Angew. Chem.* **2002**, *114*, 1442–1444; *Angew. Chem. Int. Ed.* **2002**, *41*, 1384–1386.

[8] J. A. J. Jarvis, A. F. Wells, *Acta Crystallogr.* **1960**, 13, 1027–1028.

[9] a) M. Sturm, F. Bromdl, D. Engel, W. Hoppe, *Acta Crystallophgr. Sect. B*, **1975**, *31*, 2369–2378; b) F. Seel, J. Rodrian, *J. Organometal. Chem.* **1969**, *16*, 479–484.

[10] R. Lehnert, F. Z. Seel, *Anorg. Allg. Chem.* **1980**, *464*, 187.

[11] A. Bencini, C. Benelli, D. Gatteschi, C. Zanchini, *Inorg. Chem.* **1986**, 25, 398–400.

[12] S. J. Rettig, A. Storr, D. A. Summers, R. C. Thompson, J. Trotter, *J. Am. Chem. Soc.* **1997**, *119*, 8675–8680.

[13] a) M. Inoue, M. Kishita, M. Kubo, *Inorg. Chem.* 1965, *4*, 626; b) *Bull. Chem. Soc. Jpn.* **1966**, *39*, 1352.

[14] B. Moulton, M. J. Zaworotko, *Chem. Rev.* **2001**, *101*, 1629–1658.

[15] a) M. O'Keeffe, M. Eddaoudi, H. Li, T. Reineke, O. M. Yaghi, *J. Solid State Chem.* **2000**, *152*, 3–20; b) M. O'Keeffe, N. E. Brese, *Acta Crystallogr.* **1992**, *A48*, 663–669.

[16] L. B. McCusker, *Comprehensive Supramolecular Chemistry, Vol. 7* (Chap. 14), Elsevier, **1996**, 393–423.

[17] a) Crystal data of **2′** ($[Co(im)_2{\cdot}^1/_8H_2O]$): a = 17.775(4), b = 27.617(6), c = 8.8830(18) Å, V = 4360.5(15) Å^3, Z = 16, space group *Fdd*2, Flack c = 0.03(6), GooF = 1.067, R_1 = 0.0572, wR_1 = 0.1545. b) Crystal data of **3′** ($[Zn(im)_2{\cdot}H_2O]$): $a = b$ = 22.874(3), c = 12.941(3) Å, V = 6771.0(19) Å^3, Z = 8, space group $I4_1$, GooF = 1.070, R_1 = 0.0846, wR_1 = 0.2246.

[18] a) R. L. Carlin, *Magnetochemistry*, Springer, New York, **1986**, p. 65–67 and p. 155–157; b) R. L. Carlin, *Magnetochemistry*, Springer, New York, **1986**, p. 156; c) R. L. Carlin, *Magnetochemistry*, Springer, New York, **1986**, p. 148–150; d) H. Lueken, *Magnetochemie*, Teubner Studienbucher Chemie, Leipzig, **1999**, p. 253.

[19] a) M. E. Fisher, *Proc. R. Soc. London A*, **1960**, *245*, 66; b) M. E. Fisher, *Philos, Mag.*, **1962**, *7*, 1731.

[20] D. W. Engelfriet, W. L. Groeneveld, H. A. Groenendijk, J. J. Smit, G. M. Nap, *Z. Naturforsch. Teil A* **1980**, *35*, 115–128.

[21] See, for example: a) O. R. Evans, R.-G. Xiong, Z. Wang, G. K. Wong, W. Lin, *Angew. Chem.* **1999**, *111*, 557–559; *Angew. Chem. Int. Ed.* **1999**, *38*, 536–538; b) J. Sun, L. Weng, Y. Zhou, J. Chen, Z. Chen, Z. Liu, D. Zhao, *Angew. Chem.* **2002**, *114*, 4651–4653; *Angew. Chem. Int. Ed.* **2002**, *41*, 4471–4473.
[22] L. Carlucci, G. Ciani, D. M. Proserpio, A. J. Sironi *Chem. Soc. Chem. Commun.* **1994**, 2755–2756.
[23] a) H.-L. Sun, B.-Q. Ma, S. Gao, G. Su, *Chem. Commun.* **2001**, 2586–2587; b) F. Lloret, M. Julve, J. Cano, G. D. Munno, *Mol. Cryst. Liq. Cryst.* **1999**, *334*, 569.
[24] C. Kittel, *Introduction to Solid State Physics*, Wiley, New York, **1971**.
[25] J. L. Manson, C. R. Kmety, Q.-Z. Huang, J. W. Lynn, G. M. Bendele, S. Pagola, P. W. Stephens, L. M. Liable-Sands, A. L. Rheingold, A. J. Epstein, J. S. Miller, *Chem. Mater.* **1998**, *10*, 2552–2560.
[26] $[Cd(im)_2]_\infty$(**6**): $a = 9.931(2)$, $b = 10.739(2)$, $c = 14.622(3)$ Å, $V = 1559.4(5)$ Å^3, $Z = 8$, space group *Pcab*, $R1 = 0.0296$, $wR = 0.0732$.
[27] G. M. Sheldrick, *SHELXTL-Plus V5.1 software Reference Manual*, Bruker AXS Inc., Madison, WI. **1997**.
[28] H. C. Flack, *Acta Crystallogr. Sect. A* **1993**, *39*, 876–881.

Received: March 12, 2003 [F4957]

